International Journal of Pharmaceutics 389 (2010) 122–129

Contents lists available at ScienceDirect

International Journal of Pharmaceutics

journal homepage: www.elsevier.com/locate/ijpharm

Super-short solid silicon microneedles for transdermal drug delivery applications

Li Wei-Ze[a], Huo Mei-Rong[a], Zhou Jian-Ping[a,*], Zhou Yong-Qiang[a], Hao Bao-Hua[b], Liu Ting[b], Zhang Yong[a]

[a] College of Pharmacy, China Pharmaceutical University, Nanjing 210009, PR China
[b] School of Science and Life, Northwest University, Xi'an 710069, PR China

ARTICLE INFO

Article history:
Received 23 October 2009
Received in revised form
16 December 2009
Accepted 15 January 2010
Available online 22 January 2010

Keywords:
Super-short microneedles
Scraping
Macroneedle
Galanthamine
RT-PCR
Infection

ABSTRACT

In this study, the super-short microneedles with a length of 70–80 μm were fabricated using silicon wet etching technology. As evident from the visual inspection of pierced human skin, appearance of blue spots array after Evans Blue (EB) application indicated that the super-short microneedles were able to pierce into skin by pressing and swaying against the microneedles backing layer continually with a finger. The micro-conduits created in skin were validated by histological examination.

Transport studies revealed that: (i) skin pretreated with super-short microneedles resulted in a remarkable enhancement of the galanthamine (GAL) transport, and the permeated amount increased as the insertion force increased; (ii) the super-short microneedles with flat tips were better than that with sharp tips for enhancing skin permeability; (iii) the longer time of super-short microneedles detained in skin resulted in a higher increase of skin permeability; (iv) there was no linear correlation between the GAL permeated through skin and the number of microneedles. The EIIIA$^+$ (526 bp) segment, a very sensitive marker of tissue injury, did not expressed in the skin pierced by super-short microneedles. Meanwhile, the skin pretreated with super-short microneedles did not infected after incubation with the *Staphylococcus aureus*. These results suggest that super-short microneedles may be a safe and efficient alternative for transdermal drug delivery of hydrophilic molecules.

1. Introduction

Transdermal drug delivery system (TDDS) has many advantages, such as avoiding drug degradation and metabolism in the gastrointestinal tract and liver, however, drugs must pass through the various layers of the skin to reach the systemic circulation and maintain effective concentration. The stratum corneum (SC), a main rate-limiting layer for TDDS, severely limits diffusion of most compounds especially hydrophilic molecules across skin. It varies in thickness from 10 to 40 μm and consists of adherent dead cells and thickened, cross-linked sub-plasma membrane protein "envelopes" encased in pericellular lipids (Elias, 1989). A novel method to overcome the skin's barrier is based on the formation of micropores in the SC by the use of an array of small needles, i.e. microneedles which acts as a bridge between the user-friendliness of patches and the broad effectiveness of hypodermic needles. Microneedles would protrude the SC and reach the viable epidermis to increase skin permeability or for carrying drug into skin as a coating. Over the past few years, a variety of geometries and different materials of microneedles have been made adopting the technologies of the microelectronics industry, such as arrays of silicon, metal and polymers (PLA, Polyimide, SU-8, Parylene and Polycarbonate), with sizes ranging from sub-micron to millimeters (Verbaan et al., 2007; Harvinder and Mark, 2007; Griss et al., 2001; Rodriguez et al., 2005; Seiji et al., 2007). Silicon is attractive as a common microelectronics industry substrate with extensive processing experience, especially for its biocompatible (Rebecca et al., 2002).

The microneedles can be solid or hollow. Hollow microneedles facilitate fluidic drug transport through the needles and reach into the lower epidermis (Stoeber and Liepmann, 2000). Solid microneedles have been used to pierce the skin, after which has increased skin permeability in vitro by up to several orders of magnitude for compounds ranging from small molecules to macromolecules such as peptides, proteins, DNA, and RNA (Yukako et al., 2006; Georg et al., 2006; Mikszta et al., 2002; Cormier et al., 2004), even the nanospheres (Chabri et al., 2004; McAllister et al., 2003). The microneedles with a length of less than 300 μm have been shown not be able to pierce into human skin unless using a high velocity insertion device, because of the soft underlying tissue and the elastic nature of the skin (Martanto et al., 2006a; Mukerjee et al., 2004;

* Corresponding author. Tel.: +86 25 83271272; fax: +86 25 83301606.
E-mail address: zhoujpcpu09@163.com (Z. Jian-Ping).

0378-5173/$ – see front matter © 2010 Elsevier B.V. All rights reserved.
doi:10.1016/j.ijpharm.2010.01.024

Martanto et al., 2006b; Yoshimitsu et al., 2006). However, recent studies have shown that when the length of the microneedles was long enough to pierce into the SC, the length would not effect the penetration of compounds obviously (Verbaan et al., 2007, 2008; Yukako et al., 2006).

As the thickness of SC and live epidermis are 10–40 and 50–100 μm, microneedles with a length of 70–80 μm were made and used in this study to determine the feasibility to enhance the transport of galanthamine (GAL), a hydrophilic molecule across skin. Until now, there are no previous reports on this kind of shorter microneedles used in enhancing the drug transport across skin. Because greatly short length, it was called "super-short microneedles" in our laboratory. Meanwhile, the needle with a length of 1500 μm was also fabricated for comparison. As 1500 μm is much longer than 70–80 μm, this needle was called "macroneedle" relatively in our study.

In order to effectively determine the injury of the skin caused by super-short microneedles, RT-PCR of EIIIA$^+$ (526 bp) segment was studied (Jarnagin et al., 1994; Ongenae et al., 2000; Tominaga et al., 2001; Singh et al., 2004) and the pierced skin infected with *Staphylococcus aureus* was also evaluated in this study. Abrasion (scraping) and acupuncture by stimulating some special skin points to produce striking therapeutic effects are extensively used in clinical treatment of Traditional Chinese Medicine. In fact, the action of the tools of scraping or acupuncture is not only abrading and puncturing, but also accompanied by other motion such as swaying and twisting. In fact, it is impossible for people to use microneedles only vertically piercing, however, it is very possible that the vertically piercing accompanied by swaying or turning. Therefore, the characteristics of super-short microneedles piercing into skin by pressing and swaying against the microneedles backing layer continually with a finger were also investigated.

2. Materials and methods

2.1. Materials

Galanthamine (GAL, molecular formula: $C_{17}H_{21}NO_3$; molecular weight: 287.35) were purchased from Xiaocao Co. Ltd (Shanxi, China). RNA extract kit was bought from Promega (USA). Male newly born SD (age: 7 days) and HWY/Slc hairless rats (age: 60 days) were obtained from The Fourth Military Medical University (Shanxi, China). Silicon wafer were kindly provided by Hao Bao-Hua (Northwest University, China). All other materials used were of reagent grade and were used as received. Animal experiments were conducted under the guidelines of the Life Science Research Center at China Pharmaceutical University.

2.2. Super-short microneedles and macroneedle fabrication

The super-short microneedles were designed on the basis of SIMODE simulation software, which simulates wet etching of silicon using KOH. Microneedles were fabricated by using a series of photolithography, thin-film deposition, and reactive ion etching techniques using single-crystal Si. The first process step is the deposition of nitride on a pad oxide layer using the standard well-known process of low pressure chemical vapour deposition. After deposition and patterning of square oxide patterns on a Si substrate, the portion of the Si wafers not covered by these patterns is etched away by an isotropic-reactive ion etching process. The microneedles arrays were fabricated using 30% KOH at 80 °C. The etch rate was 1.10–1.15 mm/min. When a certain tip shape formed, the microneedle body was formed by using the anisotropic Bosch process. A thin silicon nitride film was deposited to ensure biocompatibility (Wilke et al., 2005; Xie et al., 2005). The microneedle arrays were affixed to an adhesive patch comprised of a low-density polyethylene backing with a polyisobutylene adhesive. The adhesive served to hold the microneedles firmly against the skin by compensating for the mechanical mismatch between the flexible skin tissue and the rigid microneedles substrate. The super-short microneedles were imaged by scanning electron microscopy (Hitachi 3500 H, Tokyo, Japan).

Macroneedle in our study was formed by insetting an acupuncture pin in a minipore of a basement at a predetermined length of 1500 μm and fixed by adhesive. Subsequently, the extra fraction of pin was carefully cut from the back of the basement and a certain length of macroneedle was obtained.

2.3. Imaging super-short microneedle insertion into hairless rat skin

To image the formed micro-conduits after super-short microneedles insertion into skin, the full-thickness skin of hairless rats was used. Histological examination of skin samples was conducted on paraffin sections. After chemically fixing and dehydrating, the skin samples were stained with HE (hematoxylin and eosin) and sliced into 5-μm thick sections (Cryo-star HM 560 MV, Microm, Waldorf, Germany) and then viewed by bright-field microscopy (E600, Nikon, Tokyo, Japan).

2.4. Diffusion studies

In order to investigate the ability of physical pretreatment of super-short microneedles piercing for increasing skin permeability of GAL, abdominal full-thickness hairless rat skin was used. Rats were killed by diethyl ether inhalation and the abdominal skin was excised, and then thoroughly washed with the physiological saline, dried and excess subcutaneous fat was carefully eliminated. In order to protect the microneedles from damaging, the skin stretched tightly on a Styrofoam support.

In vitro transport studies were performed after the skin SC side pretreated with four experiment schedules: (1) Sharp tipped super-short microneedle arrays (10 × 10) were pierced into skin at the pressure of different force (1.0, 3.0, 5.0, 7.0 and 8.0 N), left in place for 1 min, and removed. (2) Sharp tipped and flat tipped super-short microneedle arrays (10 × 10) were pierced into skin at the pressure of 7.0 N, left in place for 1 min, and removed. (3) Flat tipped super-short microneedle arrays (10 × 10) were pierced into skin at the pressure of 7.0 N, left in place for different time (0, 0.5, 1.0, 1.5 and 2.0 min), and removed. (4) Three flat tipped super-short microneedle arrays (8 × 8, 10 × 10 and 12 × 12) were pierced into skin at the pressure of 7.0 N, left in place for 1 min, and removed. The microneedles pretreated skin by pressing and swaying against the backing layer continually with a finger; the pressure controlled by the ergograph and the schematic diagram is depicted in Fig. 1. The technique was practiced at length in order to limit the absolute error of the pressure to 20%. The skin without any treatment was used as control. Every experiment was repeated 3 times.

The side-by-side diffusion cells with the diffusion area of 2.26 cm^2 and volume of 20 ml were used. The pretreated or no treated skin was immediately placed between the donor and receptor compartments with the SC side facing the donor compartment. The acceptor phase was 15 ml physiological saline and was kept at 37 °C resulting in a skin temperature of 32 °C in the diffusion cell. The donor phase physiological saline (15 ml) contained 0.5% (w/w) GAL; 0.1 ml of the supernatant of the acceptor phase was removed for analysis at the predetermined time and replaced with fresh medium. The withdrawn supernatant was analyzed for drug content using HPLC assay method.

The amount of GAL was determined by injecting 20 μl of sample into a HPLC system (Shimadzu LC-10A, Kyoto, Japan) equipped with a UV detector (Shimadzu SPD-10A), and a

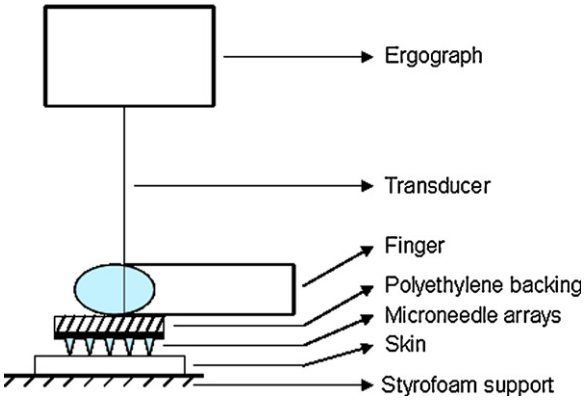

Fig. 1. The schematic diagram of super-short microneedles piercing skin by hand.

reversed phase column (NUCLEOSIL C_{18}, 5 μm, 4.6 mm × 125 mm, Chemco Scientific Co. Ltd., Osaka, Japan). The mobile phase was methanol:water:triethylamine (40:60:0.2), and phosphoric acid was used to adjust the pH to 6.4. The flow rate was 1.0 ml/min and the column temperature was 36 °C. The GAL was detected at 289 nm. The standard curve of drug in the dissolution medium was linear over 5.0–60.0 μg/ml. The detection limit was 2.0 μg/ml.

2.5. Piercing of human skin and visual inspection in vivo

The ability of the super-short microneedles to create micropores in the SC was assessed by applying onto volunteer's forearms skin. The effects of scraping and macroneedle puncture were also evaluated for comparison. The Evans Blue (EB) is a dye that has been using in clinical test for the estimation of plasma volume was used as a marker of the formation of micropores in skin (Wolman et al., 1981), for the SC is the main barrier layer against the dye permeates into skin. Three volunteers with healthy skin conditions between the age of 22 and 30 years participated in this study. The human studies obtained approval of Ethical Committee of China Pharmaceutical University.

Prior to treating, skin was carefully wiped with 70% ethanol, the needles and abrasion tool of buffalo horn slice were sterilized by immersion in 70% ethanol for 15 min. Then flat tipped super-short microneedle arrays (10 × 10) were inserted into skin by hand at the force of approximately 7.0 N for 1 min; a single macroneedle was inserted into skin by pressing and twisting at the force of approximately 7.0 N for 1 min. In order to maintain consistent scraping strength of approximately 7.0 N, the technique was practiced at length until reaching an acceptable repeatability; subsequently skin surface was abraded for 1 min. Then the treated skin was covered with 0.4% EB in physiological saline, after 30 min the excess dye was removed by washing. The presences of micropores in skin were visualized by the appearance of blue dots array on skin surface and imaged by digital camera, COOLPIX 5000 (Nikon Co. Ltd, Tokyo, Japan).

2.6. Infecting of pierced SD rats with S. aureus

Studies have suggested that microneedles could mechanically produce conduits through the SC (Verbaan et al., 2007; Cormier et al., 2004; Tao and Desai, 2003; Park et al., 2005), whether the formed conduits in skin facilitate pathogenic microorganism into body via the skin. The newly born SD rats back skin were treated with flat tipped super-short microneedles, abrasion and macroneedle at the force of 9.0 N for 2 min. Before the treatment, microneedles (10 × 10), macroneedle and abrasion tool were sterilized by immersion in 70% ethanol for 15 min.

The microneedles were inserted by using hand pressing and swaying, macroneedle pierced 100 times in 1 cm^2 evenly and abrasion carried out in 1 cm^2. After the administration, 300 μl dilution of *S. aureus* culture solution was dropwised on the treated site. At 24 h, the blood samples were collected from eye sockets and analyzed by blood cytoanalyze (CELL-DYN® 1200, USA). Then the infection judged by detecting the white blood cell (WBC), leukomonocyte (LY) and neutrophile granulocyte (NG). The rats without any treatment were used as control.

2.7. Fibronectin (FN) RT-PCR

Fibronectin secreted by fibroblasts plays a key role in the course of wound healing. The alternative splicing segments of fibronectin–EIIIA and EIIIB not expressed in normal skin tissue, however, the mRNA level of FN, EIIIA and EIIIB increase when skin damaged and show up a gradually increasing tendency. At the same condition EIIIA is more sensitive than EIIIB to the injury of skin. Therefore, the EIIIA was used as a sensitive marker for estimation the injury of skin in this study. Newly born SD rats back skin was carefully wiped with 70% ethanol and deionized water. Subsequently, the skin was pierced for 2 min by flat tipped super-short microneedle arrays (10 × 10) using hand pressing and swaying at the pressure of approximately 9.0 N. At 3, 9, 12, 16 and 24 h after the administration, the treated skin was excised under anesthesia by i.p. injection of sodium pentobarbital (50 μg/g).

In order to extract the total RNA, the excised skin samples were homogenized with 2 ml of PBS. The reverse transcription polymerase chain reaction (RT-PCR) was conducted to amplify the expressed segments, and then detected by agarose gel electrophoresis. The length of the amplified production of RT-PCR is 526 bp when they expressed the EIIIA segment (EIIIA$^+$); on the contrary, the length is 256 bp. The expressed EIIIA$^+$ (526 bp) segments can be detected by the appearance of the bright bond at the corresponding station on the agarose gel electrophoresis.

The skin which pierced with a single macroneedle for 100 times in 1 cm^2 evenly at the pressure of 9.0 N was used as a positive control. Prior to piercing, these needles were sterilized by immersion in 70% ethanol for 15 min. EIIIA-FN segment primer was synthesized by Beijing Aoke Biotechnology Company and other operations were carried out according to the instructions of RNA extract kit.

2.8. Statistics

All results are presented as means with respective standard error of the mean. Statistical analysis was carried out employing the Student's unpaired *t*-test using the software PRISM (Graph Pad). The cumulative amount of drug permeated through a unit area of skin was plotted as a function of time. Statistical differences were assumed to be reproducible when $P < 0.05$.

3. Results and discussion

3.1. Fabrication of super-short microneedles

The super-short solid silicon microneedle arrays (8 × 8, 10 × 10 and 12 × 12) were successfully fabricated. An intact sharp tipped super-short microneedle is depicted in Fig. 2A. The length of a single microneedle is about 75 μm. One flat tipped super-short microneedle is depicted in Fig. 2B, and with a length of 80 μm. Fig. 2C shows an angled view of a flat tipped super-short microneedles array. The super-short microneedles used in this study have fixed array areas, so different super-short microneedles number resulting in different microneedle density. Fig. 2B is the SEM image of a flat tipped super-short microneedle, although it seems has a relative larger

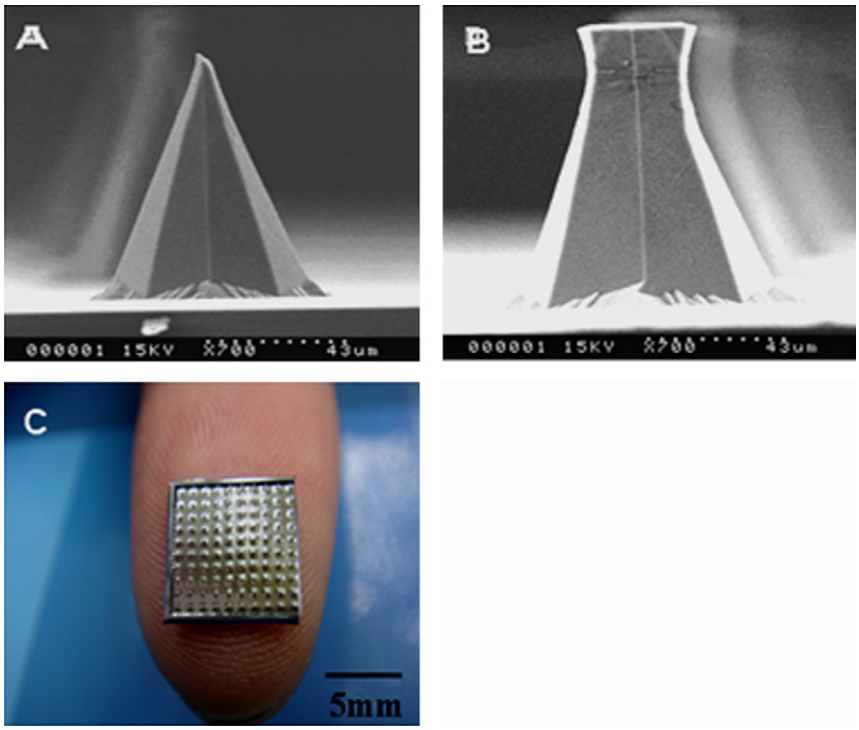

Fig. 2. The super-short microneedles used in this study, SEM images of (A) a single sharp tipped super-short microneedle and (B) a single flat tipped super-short microneedle. (C) An angled view of a flat tipped super-short microneedles array.

flat tip in width. However, as shown in Fig. 2C the flat tips of super-short microneedles are still small and sharp enough for piercing skin when compared with fingerprint.

3.2. Diffusion studies

3.2.1. Effect of insertion force on the skin permeation of GAL

Fig. 3 shows that the permeated amount of GAL significantly increased with the enhancement of insertion force from 1.0 to 5.0 N compared to the control group, indicating that super-short microneedles were able to pierce into skin by using hand pressing and swaying, and the skin barrier function obviously decreased with the increase of insertion force. It also shows that GAL did not easily penetrate skin by passive diffusion, although it is a relatively small molecule. It is noticed in Fig. 4 that piercing of the skin with different insertion force resulted in the formed micro-conduits with different diameter and depth, which indicated again that the piercing skin with different insertion force would cause different skin permeability. All of these results suggested that microneedles with lengths of 70–80 μm by using hand pressing and swaying had pierced into skin and created conduits for transport of the GAL across skin. However, as the insertion force exceeded 5.0 N the permeated GAL did not increase obviously any more, so there was no significant statistical difference among the groups of 5.0, 7.0 and 8.0 N (Student's *t*-test, $P > 0.05$), indicating that as long as the insertion force was strong enough to insert microneedles into skin, the insertion force would not significantly affect the transport enhancing properties of the super-short microneedles. In the course of diffusion studies, there were not any breaking of the super-short microneedles when pierced skin using hand (inspected by in vitro light microscopy and date not shown), indicating that they are strong and are not damaged easily, and therefore have the ability to be reused in in vitro studies.

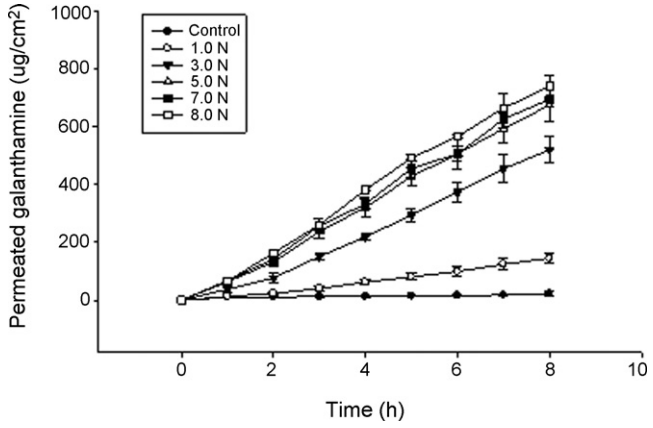

Fig. 3. Transport of GAL after skin pretreated by sharp tipped super-short microneedle arrays (10 × 10) with different insertion force. Each point represents the mean ± SD ($n = 3$).

3.2.2. Effect of tip shapes on the skin permeation of GAL

As shown in Fig. 5, GAL did not easily penetrate untreated skin, although it is a relatively small hydrophilic molecule. However, flat tipped and sharp tipped super-short microneedles were greatly improved skin permeability of GAL through hairless rat skin. The difference in the permeated amount of GAL between the two groups was statistically significant (Student's *t*-test, $P < 0.05$), the group which treated by flat tipped super-short microneedles are better than that treated by sharp tipped super-short microneedles for facilitating GAL across skin. These results suggest that the great decreasing the skin barrier function by flat tipped super-short microneedles piercing, the effective transdermal permeation pathway, especially for hydrophilic drug molecules, may be produced in skin. As shown in Fig. 6A and B were the conduits formed by flat tipped super-short microneedles piercing which have a similar outline form of a single flat tipped super-short microneedle, and no obvious folding of the skin. However, C and D show the conduits formed by sharp tipped super-short microneedles piercing, and dif-

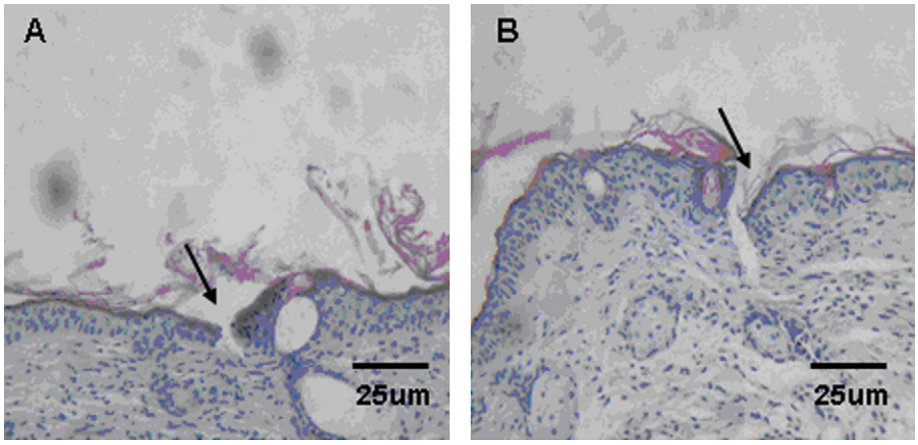

Fig. 4. Histological sections of hairless rat skin which pierced by sharp tipped super-short microneedle arrays, at different insertion force: (A) 3.0 N and (B) 7.0 N. The pierced sites tagged by arrows.

ferent skin folding was observed. The skin's folding would decrease the ability of transdermal drug delivery of the formed conduits, indicating that the conduits which formed by flat tipped microneedles without skin's folding were more effective in enhancing skin permeability. These results suggest that the flat tipped super-short microneedles have superior piercing properties compared to sharp tipped super-short microneedles.

3.2.3. *Effect of retention time on the skin permeation of GAL*

To determine whether the time of super-short microneedles detained in skin has an influence on the skin permeability of GAL, the microneedles were pierced into skin, left in place for different time, and removed. It is clearly demonstrated in Fig. 7 that the permeated GAL greatly increased with the increase of retention time compared to the control group. However, the permeated amounts of GAL were not statistically different as the retention time exceeded 1.0 min (Student's *t*-test, $P > 0.05$). This indicating that the skin permeability enhanced with the increase of retention time, as the retention time exceeded 1.0 min they would not significantly affect the transport ability of the produced conduits in skin. This might be explained by the fact that skin just likes elastic body which can generate reversible elastic deformation when pressure is exerted on it and recover as the pressure withdrawn. The shorter the persistent period of pressure exerted on skin the faster the recovery of the skin's reversible elastic deformation. However, with the persistent period prolonging, the happened reversible deformation would gradually converted into plastic deformation which a kind of irreversible deformation state and would sustain longer. As a result, the microneedles pierced into skin and left in place for a shorter time, the crushed skin around microneedles would quickly recover original shape to a maximum degree, so the formed conduits have a shorter life and lower skin permeability. While the microneedles detained in skin for a longer time induced the crushed skin around the formed conduits produced plastic deformation, this decreased the elasticity recovery of the crushed skin. Therefore the mechanically produced conduits in skin would sustain longer and caused dramatically increase of skin permeability.

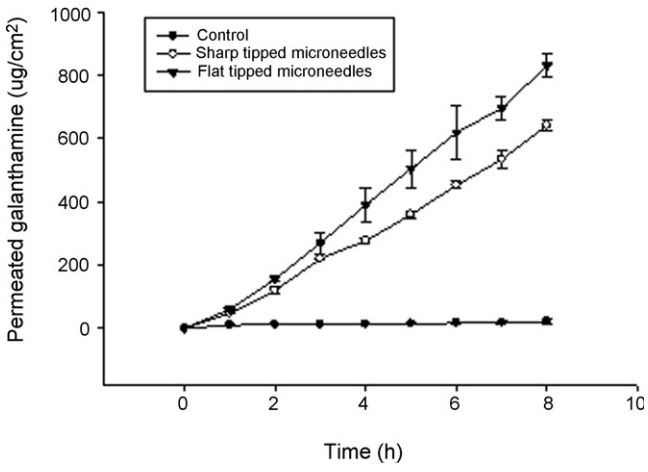

Fig. 5. Transport of GAL after skin pretreated by flat tipped and sharp tipped super-short microneedle arrays (10×10). Each point represents the mean ± SD ($n = 3$).

3.2.4. *Effect of microneedles number on the skin permeation of GAL*

The effect of microneedles number on the transport of GAL was also studied. The results in Fig. 8 show that skin permeation increased as the microneedles number increased, the fluxes of the 8×8, 10×10 and 12×12 microneedle arrays were all significantly increased compared to the untreated situation when the microneedle arrays were applied manually. The transported GAL increased with the increase of the conduits number which determined by the number of microneedles, however, there was no statistically significant difference between the groups of 10×10 and 12×12 microneedle arrays (Student's *t*-test, $P > 0.05$), although the group pretreated with the 12×12 microneedle arrays resulted in the highest transdermal transported amount. So, the increase in the number of super-short microneedles did not always result in a significantly increase in the GAL transport rate across the skin. As the same insertion force applied on different microneedle arrays resulted in different pressures at the tips of microneedles, so the pressure at one microneedle tip decreased with the increase of microneedles number. The differences in insertion force may cause differences in piercing properties as explained above, and therefore the higher density microneedles may lead to the formed conduits with small diameter. So the resulting diameter of the formed conduits in the skin may be less when using the 12×12 microneedle arrays than using the 10×10 microneedle arrays. These results demonstrated that there was no linear correlation between the microneedles number and the permeated amount of GAL, even though more conduits formed in SC by super-short microneedles piercing.

3.3. *In vivo evaluation of piercing human skin*

The piercing properties of the super-short microneedle arrays were confirmed by application of the EB on the SC side of the skin,

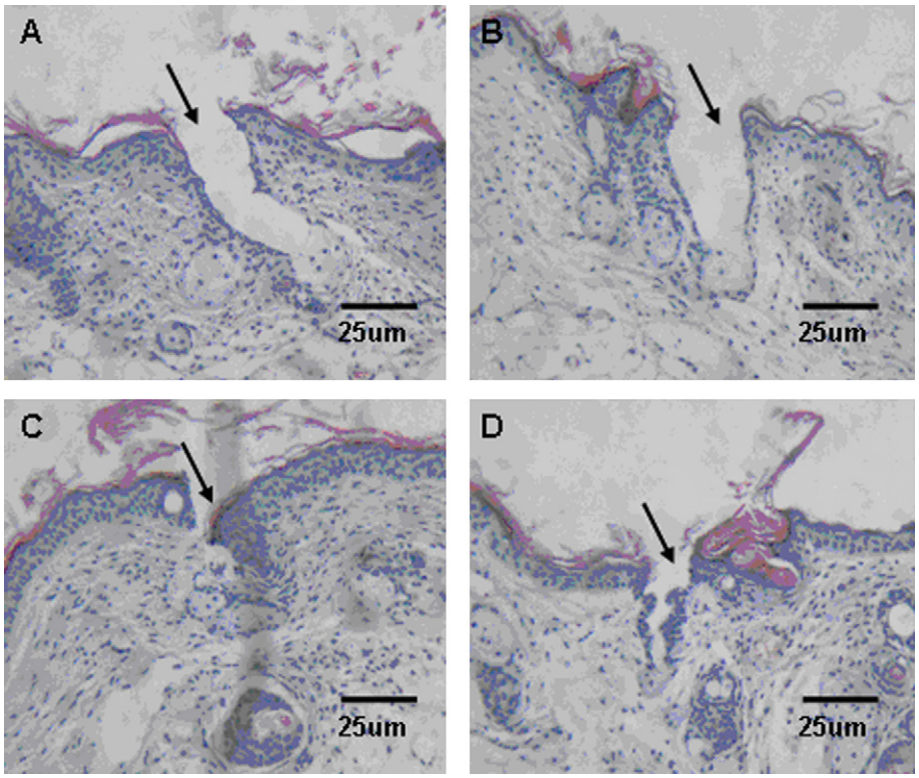

Fig. 6. Histological sections of hairless rat skin: (A and B) pierced by flat tipped super-short microneedles and (C and D) pierced by sharp tipped super-short microneedles.

and subsequent appearance of blue dots array on the skin surface corresponding to sites of super-short microneedles treated. These results indicated that the dye permeated into the skin more easily at sites where conduits formed by the microneedles piercing. Because super-short microneedles were so small that they did not reach and destroy the dermis where abundant blood capillaries located, therefore there no bleeding or swelling around the blue dots. So it is postulated that super-short microneedles of sufficient length are required to overcome the bulk elastic tissue compression of the skin, after which the microneedles are able to rupture and penetrate the skin. However, the blue spots which formed by abrasion or by macroneedle puncture were relatively large and showed up detectable bleeding and red swelling at the application site in comparison with super-short microneedles piercing.

As shown in Fig. 9, the dye diffused from the blue dots to neighbouring skin, the blue color of the skin surface changed from the thick blue to the discolored. At the 150 h after the administration, the skin treated by abrasion and macroneedle mostly renewed and the scabs began fall off. However, the skin treated by super-short microneedles still appeared a clear array of blue dots, even though the blue dots had faded. It was suggested that the micropores formed by super-short microneedles were kept much longer than that formed by abrasion and acupuncture. So the piercing of super-short microneedles would benefits transdermal drug delivery more. In addition, the subjects reported that insertion of the super-short microneedles did not cause discomfort, while the macroneedle puncture and scraping caused pain and discomfort.

3.4. Evaluation of infection of pretreated newly born SD rats

Underneath the SC, a natural defense network of potent antigen-presenting cells, the epidermal Langerhans cells and the dermal

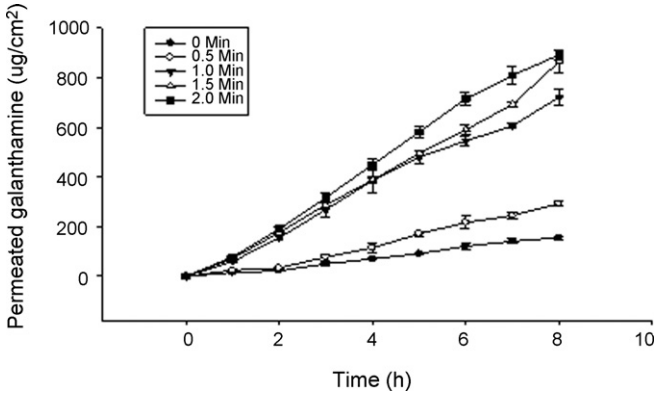

Fig. 7. Transport of GAL after skin pretreated by flat tipped super-short microneedle arrays (10 × 10) for different time. Each point represents the mean ± SD (n = 3).

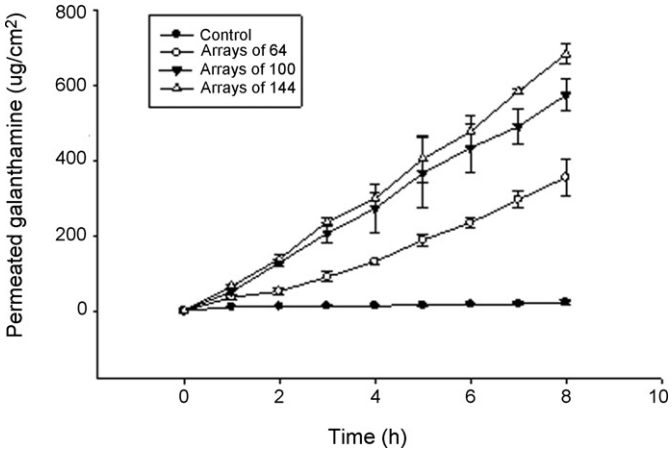

Fig. 8. Transport of GAL after skin pretreated by three super-short microneedle arrays (8 × 8, 10 × 10, 12 × 12). Each point represents the mean ± SD (n = 3).

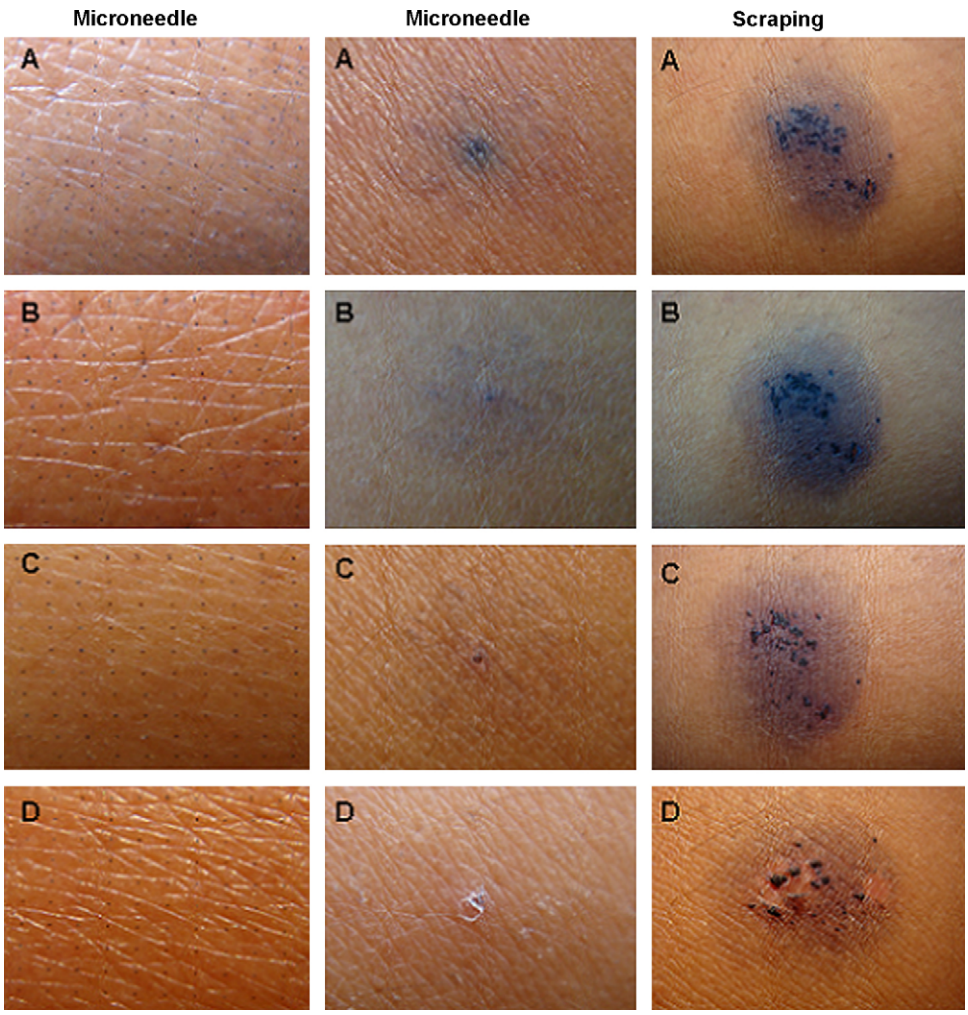

Fig. 9. Surface view of imaged healthy volunteer's forearm skin by the digital camera, after skin pretreated by super-short microneedles, single macroneedle and scraping: (A) 1 h, (B) 3 h, (C) 48 h and (D) 150 h. Piercing was visualized with the EB assay.

dendritic cells located (Yu et al., 1994). These cells readily take up foreign antigens and migrate to the draining lymph node to present antigen fragments to resting T lymphocytes, and initiate antigen-specific immune responses. Fig. 10 shows the cell population of the rats which treated by super-short microneedles was similar to that of the control group, and there was no significant difference between the two groups (Student's *t*-test, $P > 0.05$). However, the groups which treated by abrasion or by macroneedle showed up abnormal higher hemogram, indicating that the rats treated by macroneedle puncture or by abrasion were infected after the treated skin incubation with the *S. aureus*.

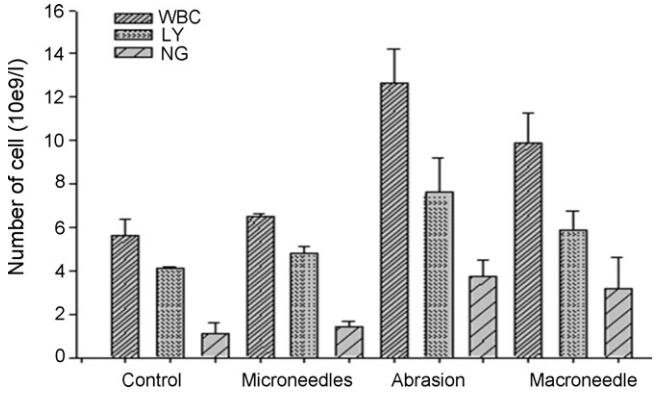

Fig. 10. The hemogram of rats pretreated with microneedles, abrasion and macroneedle. Each value represents the mean ± SD ($n = 5$).

These results implied that the breaches formed by macroneedle puncture or by abrasion were larger and deeper could cause more *S. aureus* get into body, and the formed larger breaches may be destroyed the natural defense network underneath the SC to some extent. However, the produced micro-conduits in skin by microneedles were small, in addition to the microneedle-induced conduits in the SC have a hydrophilic character and the *S. aureus* have a hydrophobic nature, this maybe caused only a few *S. aureus* could permeate into body. Because microneedles were so small that they did not reach and destroy the dermis, therefore the natural defense network underneath the skin was not damaged, they could eliminate the few traversed microorganisms. As a result, the rats treated by macroneedle puncture or by abrasion were infected and those treated by super-short microneedles were not.

3.5. Fibronectin (FN) RT-PCR of pretreated newly born SD rat's skin

Fig. 11 shows there no EIIIA$^+$ (526 bp) segments were expressed at the time of 3–24 h (2–6) after the skin of newly born SD rats pretreated with super-short microneedles by hand. While, the control group which treated by macroneedle puncture at the time of 3 h (1) obviously expressed EIIIA$^+$ (526 bp) segments. RT-PCR is a

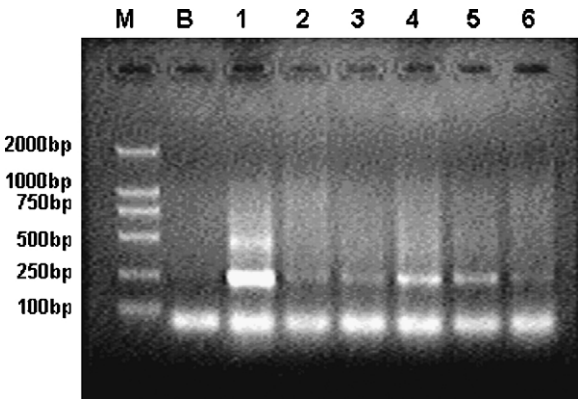

Fig. 11. Fluorescence micrograph of agarose gel electrophoresis: Maker (M), Blank (B), Control (1), 3 h (2), 9 h (3), 12 h (4), 16 h (5) and 24 h (6).

very sensitive detecting technology; it could detect the change of skin at the level of molecule. The macroneedle made in our work was significant shorter than intramuscular and hypodermic needles, so the formed pores by macroneedle were smaller than those holes induced by intramuscular and hypodermic needles. As it is known to all that intramuscular and hypodermic needles puncture do not lead to severe injury in common clinical experience, implying the damage caused by macroneedle puncture to skin should be neglected in fact, although the results of RT-PCR demonstrated that the macroneedle puncture caused skin expressed EIIIA^{+} (526 bp) segments. As the length of the macroneedle (1500 μm) much longer than that of super-short microneedles (70–80 μm), this suggested that the super-short microneedles piercing were much safer than macroneedle puncture, not to mention intramuscular and hypodermic needles puncture. So the super-short microneedles piercing would not cause any damage to skin tissue. These results are in agreement with the results obtained from the hemogram inspection after the pierced skin incubation with the *S. aureus*.

4. Conclusion

As evident from the appearance of blue spots array on skin surface after EB application and histological examination, the super-short microneedles were able to pierce into the skin and form conduits by pressing and swaying against the microneedles backing layer continually with a finger at common pressure. The created conduits in skin acted as a transdermal pathway for transport of the GAL across the skin. In vitro diffusion studies showed that the piercing of skin by using super-short microneedles greatly increased the skin permeability of GAL. Moreover, the skin permeability increased along with the increase of insertion force, retention time and microneedles number in a certain range. The super-short microneedles with flat tips were more effective than that with sharp tips in overcoming the skin's barrier properties. The super-short microneedles were so small that the skin was not damaged after they pierced into and the formed conduits in skin did not facilitate pathogenic microorganism permeate into body across the skin. In conclusion, super-short microneedles were shown to be a useful drug delivery technology for the percutaneous administration of hydrophilic molecules.

Acknowledgement

The authors would like to thank Mr. Hao for his help in fabricating of super-short microneedles.

References

Chabri, F., Bouris, K., Jones, T., Barrow, D., Hann, A., Allender, C., Brain, K., Birchall, J., 2004. Cutaneous biology microfabricated silicon microneedles for nonviral cutaneous gene delivery. Br. J. Dermatol. 150, 869–877.

Cormier, M., Johnson, B., Ameri, M., Nyam, K., Libiran, L., Zhang, D.D., Daddona, P., 2004. Transdermal delivery of desmopressin using a coated microneedle array patch system. J. Control. Rel. 97, 503–511.

Elias, P.M., 1989. The stratum corneum as an organ of protection: old and new concepts. Curr. Prob. Dermatol. 18, 10–21.

Griss, P., Enoksson, P., Tolvanen-Laakso, H.K., Merilainen, P., Ollmar, S., Stemme, G., 2001. Micromachined electrodes for biopotential measurements. J. Micromech. Sys. 10, 10–16.

Georg, W., Juanita, J., Lomi, K., Luz, L., Kofi, N., Peter, E.D., Michel, C., 2006. Effect of delivery parameters on immunization to ovalbumin following intracutaneous administration by a coated microneedle array patch system. Vaccine 24, 1653–1664.

Harvinder, S.G., Mark, R.P., 2007. Coated microneedles for transdermal delivery. J. Control. Rel. 117, 227–237.

Jarnagin, W.R., Rockey, D.C., Koteliansky, V.E., 1994. Expression of variant fibronectins in wound healing: cellular source and biological activity of the EIIIA segment in rat hepatic fibrogenesis. J. Cell Biol. 127, 2037–2048.

Martanto, W., Moore, J.S., Couse, T., Prausnitz, M.R., 2006a. Mechanism of fluid infusion during microneedle insertion and retraction. J. Control. Rel. 112, 357–361.

Martanto, W., Moore, J.S., Kashlan, O., Kahmat, R., Wang, P.M., O'Neal, J.M., Prausnitz, M.R., 2006b. Microinfusion using hollow microneedles. Pharm. Res. 23, 104–113.

McAllister, D.V., Wang, P.M., Davis, S.P., Park, J.H., Canatella, P.J., Allen, M.G., Prausnitz, M.R., 2003. Microfabricated needles for transdermal delivery of macromolecules and nanoparticles: fabrication methods and transport studies. Proc. Natl. Acad. Sci. U.S.A. 100, 13755–13760.

Mikszta, J.A., Alarcon, J.B., Brittingham, J.M., Sutter, D.E., Pettis, R.J., Harvey, N.G., 2002. Improved genetic immunization via micromechanical disruption of skin-barrier function and targeted epidermal delivery. Nat. Med. 8, 415–419.

Mukerjee, E.V., Collins, S.D., Isseroff, R.R., Smith, R.L., 2004. Microneedle array for transdermal biological fluid extraction and in situ analysis. Sens. Actuators A 114, 267–275.

Ongenae, K.C., Phillips, T.J., Park, H.Y., 2000. Level of fibronectin mRNA is markedly increased in human chronic wounds. Dermatol. Surg. 26, 447–451.

Park, J.H., Allen, M.G., Prausnitz, M.R., 2005. Biodegradable polymer microneedles: fabrication, mechanics and transdermal drug delivery. J. Control. Rel. 104, 51–66.

Rebecca, S., Shawgo, A.C., Richards, G., Yawen, L., Michael, J.C., 2002. BioMEMS for drug delivery. Curr. Opin. Solid State Mater. Sci. 6, 329–334.

Rodriguez, A., Molinero, D., Valera, E., Trifonov, T., Marsal, L.F., Pallar'es, J., Alcubilla, R., 2005. Fabrication of silicon oxide microneedles from macroporous silicon. Sens. Actuators B 109, 135–140.

Seiji, A., Hayato, I., Yuichi, I., Mitsuo, F., Hiroshi, O., 2007. Laser fabrication of high aspect ratio thin holes on biodegradable polymer and its application to a microneedle. Sens. Actuators B 139, 239–302.

Singh, P., Reimer, C.L., Peters, J.H., 2004. The spatial and temporal expression patterns of integrin alpha 9 beta1 and one of its ligands, the EIIIA segment of fibronectin, in cutaneous wound healing. J. Invest. Dermatol. 123, 1176–1181.

Stoeber, B., Liepmann, D., 2000. Fluid injection through out-of-plane microneedles. In: Proc. ASME MEMS Device 2000 IMECE, vol. 2, pp. 355–359.

Tominaga, K., Higuchi, K., Watanabe, T., 2001. Expression of gene for EIIIA- and EIIIB–fibronectin, fetal types of fibronectin, during gastric ulcer healing in rats. Dig. Dis. Sci. 46, 311–317.

Tao, S.L., Desai, T.A., 2003. Microfabricated drug delivery systems: from particles to pores. Adv. Drug Deliv. Rev. 55, 315–328.

Verbaan, F.J., Bal, S.M., van den Berg, D.J., Groenink, W.H.H., Verpoorten, H., Lüttge, R., Bouwstra, J.A., 2007. Assembled microneedle arrays enhance the transport of compounds varying over a large range of molecular weight across human dermatomed skin. J. Control. Rel. 117, 238–245.

Verbaan, F.J., Bal, S.M., van den Berg, D.J., Groenink, W.H.H., Verpoorten, H., Lüttge, R., Bouwstra, J.A., 2008. Improved piercing of microneedle arrays in dermatomed human skin by an impact insertion method. J. Control. Rel. 128, 80–88.

Wilke, N., Mulcahy, A., Ye, S.R., Morrissey, A., 2005. Process optimization and characterization of silicon microneedles fabricated by wet etch technology. Microelectron. J. 36, 650–656.

Wolman, M., Klatzo, I., Chui, E., Wilmes, F., Nishimoto, K., Fujiwara, K., Spatz, M., 1981. Evaluation of the dye-protein tracers in pathophysiology of the blood-brain barrier. Acta Neuropathol. (Berl.) 54, 55–61.

Xie, Y., Bai, Xu., Yunhua, G., 2005. Controlled transdermal delivery of model drug compounds by MEMS microneedle array. Nanomedicine 1, 184–190.

Yoshimitsu, J., Ito, Y., Shiroyara, K., Sugioka, N., Takada, K., 2006. Self-dissolving microneedles for the percutaneous absorption of EPO in mice. J. Drug Target. 14, 255–261.

Yukako, I., Eiji, H., Atsushi, S., Nobuyuki, S., Kanji, T., 2006. Feasibility of microneedles for percutaneous absorption of insulin. Eur. J. Pharm. Sci. 29, 82–88.

Yu, R.C., Abrams, D.C., Alaibac, M., Chu, A.C., 1994. Morphological and quantitative analysis of normal epidermal Langerhans cells using confocal scanning laser microscopy. Br. J. Dermatol. 131, 843–848.